

Enhanced Selective Oxidation of Benzyl Alcohol via *In Situ* H₂O₂ Production over Supported Pd-Based Catalysts

Caitlin M. Crombie,[∇] Richard J. Lewis,[∇] Rebekah L. Taylor, David J. Morgan, Thomas E. Davies, Andrea Folli, Damien M. Murphy, Jennifer K. Edwards, Jizhen Qi, Haoyu Jiang, Christopher J. Kiely, Xi Liu,* Martin Skov Skjøth-Rasmussen, and Graham J. Hutchings*



Cite This: *ACS Catal.* 2021, 11, 2701–2714



Read Online

ACCESS |



Metrics & More

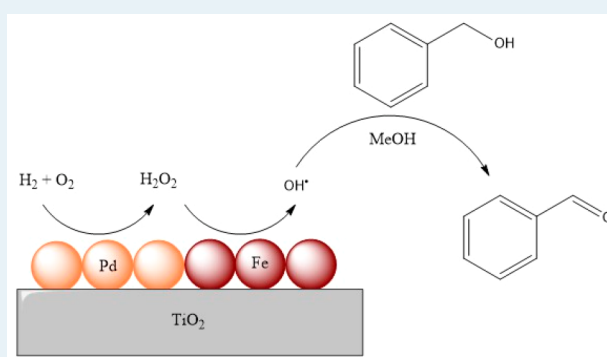


Article Recommendations



Supporting Information

ABSTRACT: Bimetallic Pd-Fe catalysts supported on TiO₂ are shown to be highly effective toward the selective oxidation of benzyl alcohol to benzaldehyde via the *in situ* production of H₂O₂ from molecular H₂ and O₂, under conditions where no reaction is observed with molecular O₂ alone. The rate of benzyl alcohol oxidation observed over supported Pd-Fe nanoparticles is significantly higher than those of either Pd-Au or Pd-only analogues. This enhanced activity can be attributed to the bifunctionality of the Pd-Fe catalyst to both synthesize H₂O₂ and catalyze the production of oxygen-based radical species as indicated by an electron paramagnetic resonance analysis. Further studies also reveal the noninnocent nature of the solvent, resulting in the propagation of radical generation pathways.



KEYWORDS: alcohol oxidation, green chemistry, hydrogen peroxide, palladium–iron, reactive oxygen species, noninnocent solvent

INTRODUCTION

The oxidation of benzyl alcohol (Scheme 1) is an often-used model reaction for the selective oxidation of alcohols, due in part to the limited number of products and the relatively well-known pathways to their formation.¹ Beyond its use as a model system, the oxidation of benzyl alcohol to the corresponding aldehyde is of great importance in its own right, with the latter finding use in the perfumery, dyestuff, and agrochemical industries.²

Typically, benzyl alcohol oxidation is carried out on an industrial scale using costly stoichiometric oxidants such as dichromate, chromic acid, and permanganate.³ However, there are concerns around atom inefficiency and the production of large quantities of undesirable, often toxic, byproducts requiring removal from product streams prior to shipping.⁴ Consequently, there is growing interest in the application of benign oxidants, such as molecular oxygen and air, through which high yields of benzaldehyde can be achieved, although typically the use of elevated reaction temperatures, in the range of 100 °C, is required.^{5–10} By comparison, the use of commercial hydrogen peroxide (H₂O₂) as an oxidant has been shown to allow significantly lower reaction temperatures to be utilized. With a range of precious^{11–13} and nonprecious-metal^{14–18} catalysts having been studied, the catalytic generation of oxygen-based radical species is widely reported to be a key step in the oxidation mechanism, with the proton abstraction of the alcohol moiety (PhCH₂OH) being crucial in

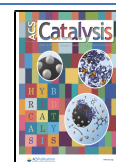
the formation of the aldehyde.^{18,19} Nevertheless, a number of drawbacks associated with the use of commercial H₂O₂ exist, namely those associated with the anthraquinone (AO) process, the means by which the vast majority (~95%) of H₂O₂ is produced on an industrial scale. Although highly efficient, the AO process is only economically viable when it is operated at a large scale, necessitating the centralization of production. Because of this, H₂O₂ is typically transported at concentrations in excess of 70 wt % prior to dilution at point of final use, effectively wasting a significant proportion of energy used in the distillation and concentration process. Furthermore, the low stability of H₂O₂ and its tendency to undergo rapid decomposition at relatively mild temperatures require the use of stabilizing agents such as acetic acid²⁰ and phosphoric acid.²¹ While the use of such additives inevitably results in additional cost to the end user, due to reactor corrosion, catalytic instability, and the need for stabilizer removal from product streams.

In principle, the *in situ* synthesis of H₂O₂ directly from H₂ and O₂ for the selective oxidation of benzyl alcohol would

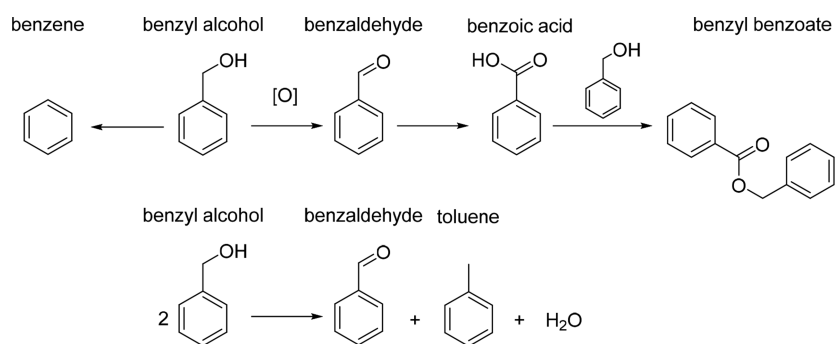
Received: October 22, 2020

Revised: February 4, 2021

Published: February 12, 2021



Scheme 1. General Reaction Pathway for Benzyl Alcohol Oxidation



avoid the numerous drawbacks associated with the use of preformed H_2O_2 , while also allowing for the application of lower reaction temperatures. Indeed, the activation of molecular O_2 through a reaction with H_2 and the *in situ* generation of oxygen-based hydroperoxyl ($-\text{OOH}$) and hydroxyl ($-\text{OH}$) species has been previously demonstrated to yield appreciable concentrations of benzaldehyde,^{8,22} with a similar approach having been reported for the selective oxidation of salicylic acid.²³

The use of supported AuPd nanoparticles has been reported to offer far greater efficacy in comparison to Pd-only analogues for a range of reactions, including the aerobic oxidation of benzyl alcohol and the direct synthesis of H_2O_2 .^{24–27} Furthermore, AuPd alloys have also been demonstrated to catalyze the *in situ* oxidation of benzyl alcohol, with high selectivities (>85%) toward benzaldehyde being typical, at temperatures where no reaction is observed using only molecular O_2 . However, conversion rates are often far below those widely reported when O_2 or air is used as an oxidant.⁸

With these previous studies in mind, we have investigated a range of bifunctional Pd-based catalysts, focusing on nonprecious alloying metals to reduce costs, for the *in situ* oxidation of benzyl alcohol utilizing H_2 and O_2 under reaction conditions where limited activity is observed with molecular O_2 and at temperatures considerably lower than those of the current industrial means of production.²⁸

EXPERIMENTAL SECTION

Catalyst Preparation. Mono- and bi-metallic 1% Pd-X/ TiO_2 catalysts (where Pd:X = 1:1 and X = Au, Mn, Fe, Co, Cu, Ni, Ce) have been prepared (on a weight basis) by an excess chloride impregnation procedure, based on a methodology previously reported in the literature.²⁹ This method has been shown to result in an enhanced dispersion of metals, in particular Au, in comparison to conventional impregnation procedures. The procedure to produce 0.5% Au–0.5% Pd/ TiO_2 (2 g) is outlined below, with a similar methodology being utilized for all mono- and bimetallic catalysts, using chloride-based metal precursors in all cases. The requisite amount of metal precursors used for the synthesis of the mono- and bimetallic catalysts is reported in Table S1.

An aqueous acidified PdCl_2 solution (1.667 mL, 6 mg mL^{-1} , 0.58 M HCl, Merck) and aqueous $\text{HAuCl}_4 \cdot 3\text{H}_2\text{O}$ solution (0.8263 mL, 12.25 mg mL^{-1} , Strem Chemicals) were mixed in a 50 mL round-bottom flask and heated to 65 °C with stirring (1000 rpm) in a thermostatically controlled oil bath, with the total volume fixed to 16 mL using H_2O (HPLC grade). When a temperature of 65 °C was reached, TiO_2 (1.98 g, EVONIK, AEROXIDE P25) was added over the course of 5 min with

constant stirring. The resulting slurry was stirred at 65 °C for a further 15 min, after which the temperature was raised to 95 °C for 16 h to allow for the complete evaporation of water. The resulting solid was mechanically ground prior to heat treatment under a reductive atmosphere (flowing 5% H_2/Ar , 500 °C, 4 h, and ramp rate of 10 °C min^{-1}).

The total metal loading of the key catalysts, as determined by EDX analysis, can be seen in Table S2, with the corresponding surface area measurements, as determined by five-point N_2 adsorption, reported in Table S3.

Catalyst Testing. *Note 1.* The reaction conditions used within this study operate below the flammability limits of gaseous mixtures of H_2 and O_2 .

Note 2. The conditions used within this work for H_2O_2 synthesis and degradation have previously been investigated, where the presence of CO_2 as a diluent for reactant gases and methanol as a cosolvent have been identified as key to maintaining high catalytic efficacy toward H_2O_2 production.^{24,30,31}

Direct Synthesis of H_2O_2 . Hydrogen peroxide synthesis activity was evaluated using a Parr Instruments stainless steel autoclave with a nominal volume of 50 mL and a maximum working pressure of 14 MPa. To test each catalyst for H_2O_2 synthesis, the autoclave was charged with the catalyst (0.01 g), the solvent (5.6 g methanol, HPLC grade, Fisher Scientific) and H_2O (2.9 g, HPLC grade, Fisher Scientific). The charged autoclave was then purged three times with 5% H_2/CO_2 (0.7 MPa) before filling with 5% H_2/CO_2 to a pressure of 2.9 MPa, followed by the addition of 25% O_2/CO_2 (1.1 MPa). The reaction mixture was stirred (1200 rpm) for 0.5 h, with the temperature being maintained at 20 °C. Reactor temperature control was achieved using a HAAKE K50 bath/circulator using an appropriate coolant. The reactor was not continuously supplied with gas. H_2O_2 productivity was determined by titrating aliquots of the final solution after reaction with acidified $\text{Ce}(\text{SO}_4)_2$ (0.01 M) in the presence of ferroin indicator. Catalyst productivities are reported as $\text{mol}_{\text{H}_2\text{O}_2} \text{kg}_{\text{cat}}^{-1} \text{h}^{-1}$.

In all cases reactions were run multiple times, over multiple batches of catalyst, with the data being presented as an average of these experiments. The catalytic activity toward H_2O_2 synthesis was found to be consistent to within $\pm 4\%$ on the basis of multiple reactions.

Degradation of H_2O_2 . The catalytic activity toward H_2O_2 degradation (via hydrogenation and decomposition pathways) was determined in a manner similar to that used for measuring the H_2O_2 direct synthesis activity of a catalyst. An autoclave was charged with methanol (5.6 g, HPLC grade, Fisher Scientific), H_2O_2 (50 wt % 0.69 g, Merck), H_2O (2.21 g,

HPLC grade, Fisher Scientific), and the catalyst (0.01 g), with the solvent composition equivalent to a 4 wt % H₂O₂ solution. From the solution, two 0.05 g aliquots were removed and titrated with acidified Ce(SO₄)₂ solution using ferroin as an indicator to determine an accurate concentration of H₂O₂ at the start of the reaction. The charged autoclave was then purged three times with 5% H₂/CO₂ (0.7 MPa) before filling with 5% H₂/CO₂ (2.9 MPa). The reaction mixture was stirred (1200 rpm) for 0.5 h, with the reaction temperature being maintained at 20 °C. After the reaction was complete, the catalyst was removed from the reaction solvents via filtration and, as described previously, two 0.05 g aliquots were titrated against the acidified Ce(SO₄)₂ solution using ferroin as an indicator. The catalyst degradation activity is reported as mol_{H₂O₂} kg_{cat}⁻¹ h⁻¹.

In all cases reactions were run multiple times, over multiple batches of catalyst, with the data being presented as an average of these experiments. The catalytic activity toward H₂O₂ degradation was found to be consistent to within ±2% on the basis of multiple reactions.

Benzyl Alcohol Oxidation via *In Situ* Production of H₂O₂. The oxidation of benzyl alcohol has been investigated in a 50 mL Parr Instruments stainless steel autoclave. The autoclave was charged with the catalyst (0.01 g), methanol (7.13 g, HPLC grade, Fisher Scientific), and benzyl alcohol (1.04 g, 9.62 mmol, Merck) along with 0.5 mL of the internal standard mesitylene (0.43 g, 3.58 mmol, Merck). The charged autoclave was then purged three times with 5% H₂/CO₂ (0.7 MPa) before filling with 5% H₂/CO₂ to a pressure of 2.9 MPa, followed by the addition of 25% O₂/CO₂ (1.1 MPa). The pressures of 5% H₂/CO₂ and 25% O₂/CO₂ were taken as gauge pressures. The reactor was subsequently heated to 50 °C, followed by stirring at 1200 rpm for 0.5 h, unless otherwise stated. The reactor was not continuously supplied with gas. After the reaction was complete, the reactor was cooled in ice to a temperature of 15 °C, after which a gas sample was taken for analysis by gas chromatography using a Varian CP-3380 instrument equipped with a TCD detector and a Porapak Q column. The product yield was determined by gas chromatography using a Varian 3200 GC instrument. The concentration of residual H₂O₂ was determined by titrating aliquots of the final solution after the reaction with acidified Ce(SO₄)₂ (0.01 M) in the presence of ferroin indicator.

In all cases reactions were run multiple times, over multiple batches of catalyst, with the data being presented as an average of these experiments. For benzyl alcohol oxidation the total product yield was observed to be consistent to within ±5% on the basis of multiple reactions.

H₂ conversion (eq 1), benzyl alcohol conversion (eq 2), product yield (eq 3), and H₂ selectivity (eq 4) are defined as follows:

$$\text{H}_2 \text{ conversion (\%)} = \frac{\text{mmol}_{\text{H}_2(t(0))} - \text{mmol}_{\text{H}_2(t(1))}}{\text{mmol}_{\text{H}_2(t(0))}} \times 100 \quad (1)$$

$$\begin{aligned} \text{benzyl alcohol conversion (\%)} \\ = \frac{\text{benzyl alcohol reacted (mmol)}}{\text{benzyl alcohol initial (mmol)}} \times 100 \end{aligned} \quad (2)$$

$$\text{product yield (\%)} = \frac{\text{product (mmol)}}{\text{benzyl alcohol initial (mmol)}} \times 100 \quad (3)$$

$$\text{H}_2 \text{ selectivity} = \frac{\text{total product (mmol)}}{\text{H}_2 \text{ conversion (mmol)}} \times 100 \quad (4)$$

It should be noted that the choice of a methanol-only solvent has been previously shown by Santonastaso et al.⁸ to lead to an enhancement in catalytic activity under reaction conditions similar to those utilized within this work. This enhancement in activity, in comparison to a water–methanol or solventless system, has been previously ascribed to the increased solubility of the reactant gases in methanol.³²

Gas Replacement Experiments for the Oxidation of Benzyl Alcohol via the *In Situ* production of H₂O₂. A procedure identical with that outlined above for the oxidation of benzyl alcohol was followed for a reaction time of 0.5 h. After this, stirring was stopped and the reactant gas mixture was vented prior to replacement with the standard pressures of 5% H₂/CO₂ (2.9 MPa) and 25% O₂/CO₂ (1.1 MPa). The reaction mixture was then stirred (1200 rpm) for a further 0.5 h. To collect a series of data points, as in the case of Figure 7, it should be noted that individual experiments were carried out and the reactant mixture was not sampled online.

Hot Filtration Experiments for the Oxidation of Benzyl Alcohol via the *In Situ* Production of H₂O₂. A procedure identical with that outlined above for the oxidation of benzyl alcohol was followed for a reaction time of 0.5 h. Following this, the stirring was stopped and the reactant gas mixture vented prior to the removal of the solid catalyst via filtration. The postreaction solution was returned to the reactor to identify the contribution of leached species to the observed activity. Further experiments were conducted, where a fresh 1% Pd/TiO₂ catalyst was added to the reaction mixture prior to running the reaction for a further 0.5 h.

Benzyl Alcohol Oxidation via Aerobic Conditions. A procedure identical with that outlined above for the oxidation of benzyl alcohol was followed for a reaction time of 0.5 h, with the reactor charged with 25% O₂/CO₂ (1.1 MPa) and N₂ (2.9 MPa). As above, the reactor was not continually supplied with gas.

Radical Trapping Experiments with Electron Paramagnetic Resonance Spectroscopy. The catalyst (0.01 g), methanol (7.13 g, HPLC grade, Fisher Scientific), and benzyl alcohol (1.04 g, 9.6 mmol, Merck) were placed in the reactor along with 0.5 mL of the internal standard mesitylene (0.43 g, 3.58 mmol, Merck) and 5,5-dimethyl-1-pyrroline *N*-oxide (12 μL, Merck). The reactor was purged three times with 5% H₂/CO₂ (0.7 MPa) and then filled with 5% H₂/CO₂ (2.9 MPa) and 25% O₂/CO₂ (1.1 MPa). The reactor was then heated to 50 °C, and once that temperature was reached, stirring (1200 rpm) was commenced for 0.5 h. Once the reaction was complete, the reactor was purged with 20 bar of N₂ for 20 min before the catalyst was separated by filtration and the filtered solution loaded into a 1.1 mm quartz tube for analysis by EPR spectroscopy.

Various blank reactions were also analyzed by EPR spectroscopy to determine any background activity.

Continuous wave X-band EPR spectra were recorded at 298 K using a Bruker EMX Micro spectrometer equipped with a Bruker ER 4123d dielectric resonator. Spectra were recorded at ca. 9.75 GHz and 2 mW microwave power, with 100 kHz field

modulation frequency, 1 G field modulation amplitude, 5×10^4 receiver gain, 10.00 ms conversion time, and 5.02 ms time constant. EPR spectra were simulated using the EasySpin toolbox³³ running within the MathWorks Matlab environment.

Catalyst Characterization. Samples for electron microscopy analysis were prepared by dry dispersion of the powder catalyst onto 300 mesh copper grids coated with a holey carbon film. Conventional transmission electron microscopy (TEM) was performed on a JEOL JEM-2100 instrument operating at 200 kV. Aberration-corrected scanning transmission electron microscopy (AC-STEM) was performed using a probe-corrected S/TEM instrument (Thermo Fisher, Themis Z), operating at 300 kV. The latter instrument was equipped with a Super-X EDS detector for high-spatial XEDS characterization.

A Thermo Fisher Themis Z probe corrected TEM instrument equipped with a Super-EDX detector, in STEM mode with a probe current of pA was used to conduct EDX analysis. Data were collected over a 500 nm^2 representative sample. Quantitative data analysis was done by using Thermo Fisher Themis Z Velox software.

A Thermo Scientific K-Alpha⁺ spectrometer was used to collect X-ray photoelectron spectra utilizing a microfocused monochromatic Al K α X-ray source operating at 72 W. Data were collected over an elliptical area of approximately $400 \mu\text{m}^2$ at pass energies of 40 and 150 eV for high-resolution and survey spectra, respectively. Sample charging effects were minimized through a combination of low-energy electrons and Ar⁺ ions, and a C(1s) line at 284.8 eV was present for all samples. All data were processed using CasaXPS v2.3.20 rev. 1.2H using a Shirley background, Scofield sensitivity factors, and an energy dependence of -0.6 . Fitting was achieved using models taken from bulk compounds (Pd and Au metal foils and PdO). The Au(4f) peaks fit on top of the Ti loss structure and also the Pd(4s) signal; to account for this background, a broad, constrained Voigt function was used to model these underlying peaks.

Brunauer–Emmett–Teller (BET) surface area measurements were conducted using a Quadrasorb surface area analyzer. A five-point isotherm of each material was measured using N₂ as the adsorbate gas. Samples were degassed at 250 °C for 2 h prior to the surface area being determined by five-point N₂ adsorption at $-196 \text{ }^\circ\text{C}$, and data were analyzed using the BET method.

RESULTS AND DISCUSSION

Our initial studies investigated the efficacy of a range of TiO₂-supported monometallic catalysts, prepared by a co-impregnation procedure,²⁹ toward the direct synthesis and subsequent degradation of H₂O₂. These experiments were carried out under conditions previously optimized to enhance H₂O₂ stability, namely in the presence of a methanol cosolvent and CO₂ gaseous diluent, both of which have been shown to inhibit H₂O₂ degradation pathways (Table S4).^{24,30} The inactivity of the monometallic catalysts toward the formation of H₂O₂ is clear, with the exception of the 1% Pd/TiO₂ catalyst ($30 \text{ mol}_{\text{H}_2\text{O}_2} \text{ kg}_{\text{cat}}^{-1} \text{ h}^{-1}$), which was expected, since supported Pd catalysts have been well studied for the direct synthesis of H₂O₂.^{34–39} As with H₂O₂ synthesis activity, only the 1% Pd/TiO₂ catalyst was observed to offer any measurable activity toward H₂O₂ degradation ($198 \text{ mol}_{\text{H}_2\text{O}_2} \text{ kg}_{\text{cat}}^{-1} \text{ h}^{-1}$) via hydrogenation and decomposition pathways. This result is perhaps more unexpected given the well-known activity of a

range of these metals, such as Fe, Mn, and Cu, to catalyze H₂O₂ decomposition to H₂O⁴⁰ and may be ascribed to the *in situ* formation of carbonic acid, through the dissolution of the CO₂ reactant gas diluent, and resulting stabilization of H₂O₂. We have previously reported the effects of CO₂ on catalytic activity to be comparable to those observed when the reaction solution is acidified to pH 4 using HNO₃.³⁰

As may have been expected given the limited activity of most of the monometallic catalysts toward H₂O₂ production, the catalytic oxidation of benzyl alcohol via the *in situ* production of H₂O₂ from H₂ and O₂ was also limited (Figure 1, with H₂

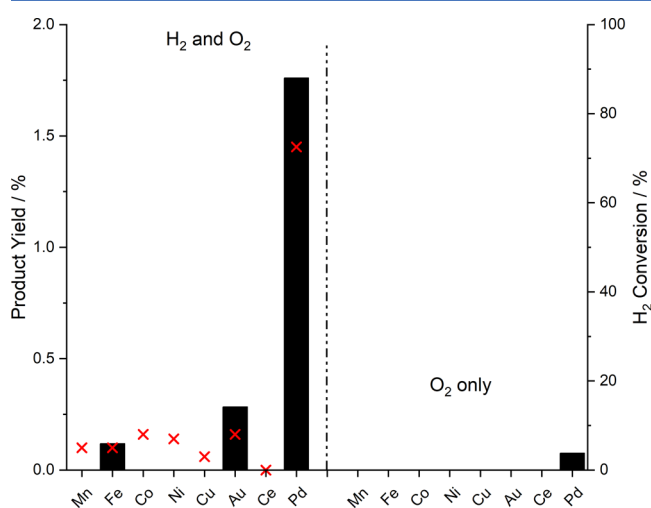


Figure 1. Comparison of the catalytic activities of TiO₂-supported monometallic catalysts toward the *in situ* oxidation of benzyl alcohol. Key; benzaldehyde (black bars); H₂ conversion (red crosses). Reaction conditions: mass of catalyst (0.01 g), benzyl alcohol (1.04 g, 9.62 mmol), MeOH (7.1 g), 5% H₂/CO₂ (2.9 MPa), 25% O₂/CO₂ (1.1 MPa), 0.5 h, 50 °C, 1200 rpm. Note: for experiments carried out using only O₂, a gaseous mixture of 25% O₂/CO₂ (1.1 MPa) and N₂ (2.9 MPa) was used.

conversion and residual H₂O₂ being presented in Table S5). Again, the only exception was the 1% Pd/TiO₂ catalyst, which was observed to offer appreciable conversion rates of benzyl alcohol to benzaldehyde (1.80% product yield). The significant improvement in benzyl alcohol oxidation in the presence of H₂ and O₂ in comparison to that observed when molecular H₂ or O₂ was used alone or when commercial H₂O₂ was used should also be noted (Figure S1). The limited activity displayed under the purely aerobic conditions used in this work are related to the low reaction temperatures employed, whereas temperatures typically exceeding 80 °C are utilized for aerobic benzyl alcohol oxidation.^{7,41,42}

In keeping with previous studies investigating both the oxidation of benzyl alcohol using molecular O₂^{7,26} and the direct synthesis of H₂O₂,^{27,43,44} the incorporation of Au into TiO₂-supported Pd nanoparticles was observed to lead to a significant enhancement in catalytic efficacy toward benzyl alcohol oxidation via *in situ* H₂O₂ production (2.80% product yield) (Figure 2), as well as H₂O₂ synthesis (Table S6). This synergistic effect observed through alloying Au and Pd is often attributed to a combination of electronic modification,⁴¹ with Au acting as an electronic promoter for Pd, and the disruption of contiguous Pd ensembles.⁴⁵

By comparison, the introduction of a range of secondary non-precious metals, such as Co and Fe, into a supported Pd

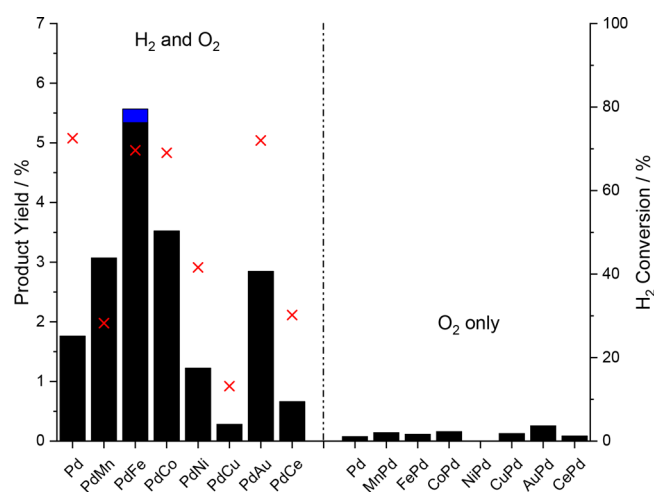


Figure 2. Catalytic activity of bimetallic Pd-X/TiO₂ catalysts toward the selective oxidation of benzyl alcohol, via *in situ* H₂O₂ synthesis. Key: benzaldehyde (black bars), benzoic acid (blue bars), H₂ conversion (red crosses). Reaction conditions: catalyst (0.01 g), benzyl alcohol (1.04 g, 9.62 mmol), MeOH (7.1 g), 5% H₂/CO₂ (2.9 MPa), 25% O₂/CO₂ (1.1 MPa), 0.5 h, 50 °C, 1200 rpm.

catalyst leads only to a minor enhancement in H₂O₂ synthesis rates, under conditions optimal for H₂O₂ production, with this being linked to an inhibition in competitive H₂O₂ degradation reactions in comparison to the 1% Pd/TiO₂ catalyst (Table S6). This observation is in keeping with numerous previous studies which report the beneficial role of alloying Pd with a range of secondary nonprecious metals, including Sn,^{46,47} Zn,⁴⁸ Ag,⁴⁹ Te,⁵⁰ Ni,^{51,52} Co,⁵³ and In,⁵⁴ with the enhanced catalytic selectivity often being attributed to a reduction in contiguous Pd ensembles and an increased number of isolated Pd sites favorable for H₂O₂ formation.⁴⁶

Interestingly, the introduction of these secondary base metals, and Fe in particular, into supported Pd nanoparticles was observed to lead to a dramatic improvement in catalytic activity toward benzyl alcohol oxidation under *in situ* conditions. Indeed, the catalytic efficacy of the 1% PdFe/TiO₂ catalyst (5.60% product yield) far exceeds that observed for the analogous 1% PdAu/TiO₂ catalyst, with near-complete selectivity toward benzaldehyde (96%). The product selectivity based on H₂ and residual H₂O₂ is summarized in Table S7, with apparent turnover frequencies being given in Table S8. Further studies, comparing the activity of the bimetallic 1% Pd-Fe/TiO₂ catalyst to that of a physical mixture of 1% Pd/TiO₂ and 1% Fe/TiO₂ catalysts, with the total moles of the metal present being consistent with the bimetallic catalyst, indicate the need for both metals to be immobilized on the same crystalline support grain in order to achieve enhanced activity (Table S9).

Table 1. Comparison of Catalytic Selectivity of the 1% Pd/TiO₂, 1% PdAu/TiO₂, and 1% PdFe/TiO₂ Catalyst Formulations toward Benzaldehyde and H₂ Conversion^a

catalyst	H ₂ conversion (%)	selectivity based on H ₂ (%)	benzyl alcohol conversion (%)	benzaldehyde selectivity (%)
1% Pd/TiO ₂	72	9	1.80	100
1% PdAu/TiO ₂	72	16	2.80	100
1% PdFe/TiO ₂	71	33	5.60	96

^aReaction conditions: catalyst (0.01 g), benzyl alcohol (1.04 g, 9.62 mmol), MeOH (7.1 g), 5% H₂/CO₂ (2.9 MPa), 25% O₂/CO₂ (1.1 MPa), 0.5 h, 50 °C, 1200 rpm.

With synergistic effects being well-known to occur upon alloying Au and Pd,⁴¹ and the evident improvement in activity when Fe is introduced into a supported Pd catalyst, we were subsequently motivated to investigate this subset of catalysts in order to gain further insight into the underlying cause for the observed differences in catalytic performance.

An assessment of catalytic selectivity toward benzaldehyde and H₂ utilization is presented in Table 1. It is apparent that all three catalysts offer similarly high selectivities toward benzaldehyde, typical of their relatively low rates of benzyl alcohol conversion. However, the H₂ selectivity (i.e., H₂ utilized in the *in situ* oxidation of benzyl alcohol) of the 1% PdFe/TiO₂ catalyst (33% H₂ selectivity) is seen to be far superior to that of either the 1% Pd/TiO₂ (9% H₂ selectivity) or 1% PdAu/TiO₂ (16% H₂ selectivity) analogue, clearly highlighting the beneficial role of Fe incorporation into Pd and to a lesser extent that of adding Au.

The catalytic selectivity of Pd-based catalysts toward H₂O₂ is known to be highly dependent on the oxidation state of Pd, with metallic Pd species typically being more active toward H₂O₂ degradation than analogous Pd²⁺-based catalysts.^{55–57} More recently a number of studies have reported the enhanced catalytic efficacy of mixed Pd⁰-Pd²⁺ domains, in comparison to Pd⁰- or Pd²⁺-rich species, for both the direct synthesis of H₂O₂^{44,58,59} and the aerobic oxidation of benzyl alcohol.⁶⁰ An analysis of our supported Pd-based catalysts via XPS (Table 2

Table 2. Effect of Secondary Metal Incorporation into the 1% Pd/TiO₂ Catalyst on Surface Elemental Compositions as Determined by XPS Analysis^a

catalyst	Pd ⁰ :Pd ²⁺	Pd:M (M = Au, Fe)
1% Pd/TiO ₂	0.92	-
1% PdAu/TiO ₂	0.90	0.67
1% PdFe/TiO ₂	0.50	0.38

^aAll catalysts were exposed to a reductive heat treatment before XPS analysis (5% H₂/Ar, 500 °C, 4 h, 10 °C min⁻¹).

and Figure S2) indicates that despite exposure to a reductive heat treatment (5% H₂/Ar, 500 °C, 4 h), upon introduction of Fe into a Pd catalyst, a significant proportion of Pd still exists as Pd²⁺ (Pd⁰:Pd²⁺ = 0.5), while Fe exists as an oxide. On the other hand, Pd is present predominantly in the metallic form in both the 1% Pd/TiO₂ and 1% PdAu/TiO₂ catalysts. It is therefore possible to attribute the enhanced selectivity of the 1% PdFe/TiO₂ catalyst, at least in part, to the formation of domains of mixed Pd oxidation states and a reduction in competitive H₂O₂ degradation pathways, although it should be noted that the Pd oxidation states of the fresh material is likely not fully representative of those under reaction conditions.

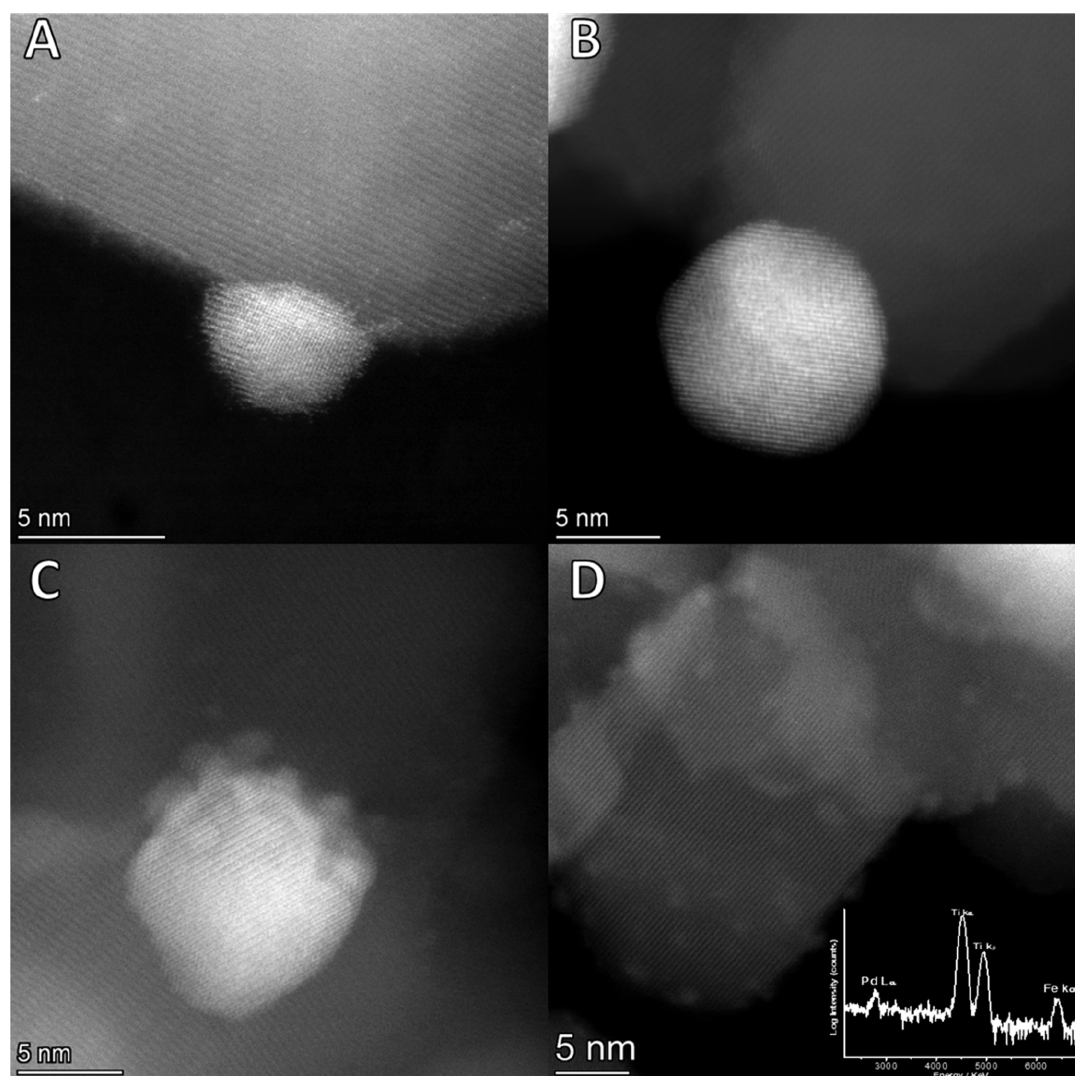


Figure 3. Representative STEM-HAADF images of the (A) 1% Pd/TiO₂, (B) 1% PdAu/TiO₂, and (C, D) 1% PdFe/TiO₂ catalyst materials. As shown in (C), the surfaces of the larger PdFe alloy particles are decorated with smaller clusters. In (D) the smaller clusters are well dispersed on the TiO₂ support. The inset X-EDS spectrum is of the area shown in (D) and indicates that the small clusters contain both Fe and Pd.

The catalytic activity toward H₂O₂ synthesis, in particular that of monometallic Pd catalysts, is widely reported to be dependent on nanoparticle size,^{36,60,61} with additional studies reporting the relationship between this metric and the catalytic efficacy toward benzyl alcohol oxidation under aerobic conditions.^{62,63} Indeed, Zhang et al. have reported that an optimal Pd particle size between 3.6 and 4.3 nm exists for the oxidation of benzyl alcohol when molecular O₂ is used as the oxidant.⁶⁴ Further detailed studies by Wang et al.⁶⁵ have elucidated the role of both geometric and electronic effects in the catalytic performance of supported Pd nanoparticles toward aerobic benzyl alcohol oxidation, with the catalytic activity and selectivity directly related to particle size. An analysis of the Pd-based catalysts by transmission electron microscopy reveals that there is a significant variation in the average metal nanoparticle size with catalyst formulation. In keeping with previous studies,²⁹ the monometallic catalyst displays Pd particles in the 3–5 nm range, with a mean size of ~4.1 nm (Figure 3A and Figures S3A,B and S4A). However, there is also evidence from HAADF-STEM imaging experiments for the coexistence of a population of smaller sub-nanometer Pd-containing clusters (Figure 3A). As determined

previously,²⁴ the alloying of Au with Pd results in an increase in mean particle size, in comparison to the Pd-only analogue. The majority of the supported PdAu particles were found to be in the 4–10 nm size range, with a mean size of 7.9 nm (Figure 3B and Figures S3C and S4B). However, some occasional larger particles, up to approximately 15 nm were also noted to be present (Figure 3D). Elemental STEM-XEDS mapping studies on individual particles, such as those presented in Figure 4A, confirmed that the PdAu particles are well-mixed random alloys, which is in agreement with what would be expected from this catalyst synthesis procedure.²⁹ In contrast, the 1% PdFe/TiO₂ catalyst displays a bimodal size distribution with much of the metal being present as small 1 nm clusters either isolated on the titania surface (Figure 3D) or decorating the surface of larger 10–20 nm metallic particles (Figure 3C and Figure S4C). XEDS elemental mapping studies (Figure 4B) confirm that these larger particles are in fact PdFe alloys. These decorated alloyed particles were relatively few in number and were very sparsely distributed over the support (Figure S3E,F). Our XEDS analysis of the smaller clusters revealed that they also contain both Fe and Pd (see inset spectra in Figure 3D).

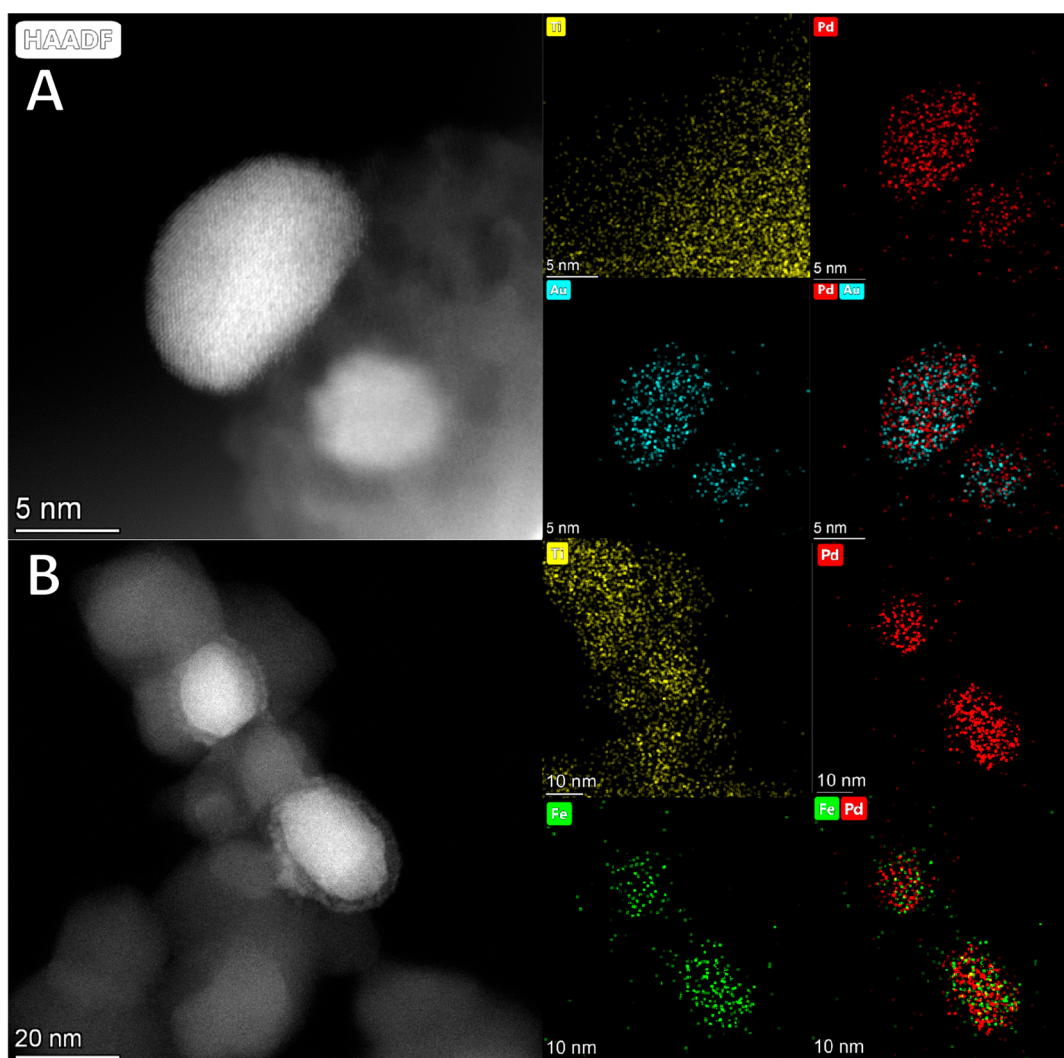


Figure 4. STEM-XEDS mapping of (A) the 1% PdAu/TiO₂ catalyst showing alloyed AuPd particles and (B) the 1% PdFe/TiO₂ catalyst showing alloyed FePd particles decorated with smaller clusters.

Time-on-line studies comparing the catalytic efficacy of the Pd-based catalysts can be seen in Figure 5 (additional data are presented in Figure SSA–C). As with our standard reaction time studies (0.5 h), the higher catalytic activity of the 1% PdFe/TiO₂ catalyst is once again clear, with a product yield of 7.3% achieved over a time period of 2 h, which is significantly greater than that of either the 1% PdAu/TiO₂ (3.7% product yield) or 1% Pd/TiO₂ (1.8% product yield) analogue, when tested over the same reaction time. The selectivity toward benzaldehyde appears to be consistent for all three catalysts, indicating that the subsequent reactions, including the production of toluene and benzoic acid, are suppressed. This is perhaps unsurprising given the previous studies by Sankar et al.⁶⁶ and Partenheimer,⁶⁷ who reported that the presence of benzyl alcohol and a range of other alcohols (although notably not methanol, which is the solvent used in this study) even at low concentrations can inhibit the further oxidation of benzaldehyde. It should be noted that the 1% PdFe/TiO₂ catalyst displays a rate of conversion under identical reaction conditions comparable to that of the 5% PdAu/TiO₂ catalyst previously reported by Santonastaso et al.,⁸ despite having a 10 times lower precious metal content.

A comparison of initial reaction rates (Table 3), at a short reaction time (5 min) where there is assumed to be no limitations associated with reactant gas availability, further highlights the increased activity of the 1% PdFe/TiO₂ catalyst. The rate of benzyl alcohol conversion over the 1% PdFe/TiO₂ catalyst was found to be 3.8 times greater than that observed for the 1% Pd/TiO₂ catalyst and 1.3 times greater than that of the analogous bimetallic 1% PdAu/TiO₂ catalyst. It should also be noted that, for all of the catalysts studied, the initial rate of the reaction is far greater than the overall rate.

Santonastaso et al.⁸ have previously investigated the efficacy of a 5% PdAu/TiO₂ catalyst for the oxidation of benzyl alcohol under reaction conditions similar to those used in this study, with a plateau in benzyl alcohol conversion being reported after relatively short reaction times (20 min), this loss of activity being attributed to catalyst deactivation. In our work, we observed a similar plateau in benzyl alcohol conversion rate over the three catalysts that we chose to study in detail. The H₂ conversion rates over the three catalysts were seen to be particularly high, being approximately 80% over 2 h on-stream (Table S10). These observations are indicative of the reaction becoming limited by H₂ availability rather than through catalyst deactivation. On the other hand, a determination of

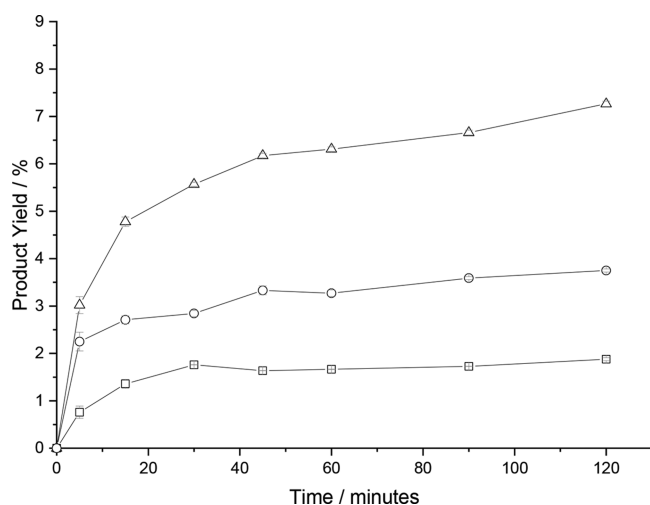


Figure 5. Comparison of the catalytic activity toward the selective oxidation of benzyl alcohol via H_2O_2 synthesis as a function of reaction time over our TiO_2 -supported mono- and bi-metallic Pd catalysts. Key: 1% Pd/ TiO_2 (squares), 1% PdAu/ TiO_2 (circles), 1% PdFe/ TiO_2 (triangles). Reaction conditions: catalyst (0.01 g), benzyl alcohol (1.04 g 9.62 mmol), MeOH (7.1 g), 5% H_2/CO_2 (2.9 MPa), 25% O_2/CO_2 (1.1 MPa), 50 °C, 1200 rpm.

Table 3. Comparison of Initial Rates of Benzyl Alcohol Oxidation over TiO_2 -Supported Mono- and Bi-metallic Pd-Based Catalysts^a

catalyst	rate of reaction ($\mu\text{mol s}^{-1}$)	benzyl alcohol conversion (%)	benzaldehyde selectivity (%)
1% Pd/ TiO_2	0.24	0.80	100
1% PdAu/ TiO_2	0.72	2.30	100
1% PdFe/ TiO_2	0.97	3.00	100

^aReaction conditions: catalyst (0.01 g), 1.04 g benzyl alcohol (1.04 g, 9.62 mmol), MeOH (7.1 g), 5% H_2/CO_2 (2.9 MPa), 25% O_2/CO_2 (1.1 MPa), 0.083 h, 50 °C, 1200 rpm.

residual H_2O_2 (i.e., H_2O_2 not consumed through degradation pathways or in the conversion of benzyl alcohol) (Table S11) reveals that, for the 1% Pd/ TiO_2 and 1% PdAu/ TiO_2 catalysts, this metric decreases substantially over the reaction time studied, with a maximum residual H_2O_2 concentration being observed after 5 min online, at 130 and 188 $\mu\text{mol}_{\text{H}_2\text{O}_2}$ for the 1% Pd/ TiO_2 and 1% PdAu/ TiO_2 catalysts, respectively. In comparison, a measurement of residual H_2O_2 over the 1% PdFe/ TiO_2 catalyst revealed that this metric was steady over 2 h, although at a far lower level (approximately 30 $\mu\text{mol}_{\text{H}_2\text{O}_2}$) in comparison to that observed over the corresponding PdAu and Pd-only catalysts. In the case of the 1% Pd/ TiO_2 and 1% PdAu/ TiO_2 catalysts, these observations may indeed be indicative of catalyst deactivation, while the enhanced activity of the 1% PdFe/ TiO_2 catalyst may result from the continual production of H_2O_2 .

XPS analysis of the three catalysts over the course of a 2 h reaction (Figure 6 and Table S12) indicates that the $\text{Pd}^0:\text{Pd}^{2+}$ ratio observed in the fresh 1% FePd/ TiO_2 material is maintained to a greater extent over extended reaction times, in comparison to that observed over the corresponding Pd-only and PdAu catalysts. For the 1% Pd/ TiO_2 catalyst, a complete shift in Pd oxidation state toward Pd^0 , most likely as a result of *in situ* reduction, is observed after 5 min on-stream, while a similar shift is effectively observed after 15 min for the

1% PdAu/ TiO_2 catalyst ($\text{Pd}^0:\text{Pd}^{2+} = 0.96$). By comparison, the presence of mixed $\text{Pd}^0\text{-Pd}^{2+}$ domains is seen to be retained over a reaction time of 90 min ($\text{Pd}^0:\text{Pd}^{2+} = 0.94$) for the 1% PdFe/ TiO_2 material. As discussed previously,⁵⁸ the presence of these mixed domains has been related to enhanced activity toward both H_2O_2 synthesis and benzyl alcohol oxidation. As such, the enhanced activity of the 1% PdFe/ TiO_2 catalyst may in part be attributed to the retention of these regions of mixed Pd oxidation states.

Given the high H_2 conversion rates observed under our standard reaction conditions and the potentially H_2 diffusion limited nature of the reaction at relatively short reaction times, we next investigated the catalytic activity over multiple sequential benzyl alcohol oxidation tests, as shown in Figure 7 (the product distribution is shown in Table S13), where gas mixtures were replenished at intervals of 0.5 h. A near-linear increase in benzyl alcohol conversion was found over all three catalysts in this experiment. This possibly indicates (i) that if catalyst deactivation does occur then it is not a permanent effect or, more likely, (ii) given the first-order dependence of H_2O_2 production with respect to H_2 , there is limited H_2 availability in the reaction.⁶⁸ Again, these sequential reaction studies clearly demonstrate the enhanced performance of the 1% PdFe/ TiO_2 catalyst in comparison to the 1% Pd/ TiO_2 and 1% PdAu/ TiO_2 analogues. Indeed, the extent of benzyl alcohol conversion over the 1% PdFe/ TiO_2 catalyst is exceptionally high (22.02%) with a near-complete selectivity (96%) toward benzyl alcohol and with limited production of either benzoic acid or toluene over four subsequent reaction runs. The activity of the 1% PdFe/ TiO_2 catalyst is seen to far exceed the rates of conversion observed over the 1% Pd/ TiO_2 (6.23%) and 1% PdAu/ TiO_2 (11.75%) catalysts, when they are tested over the same number of sequential reaction cycles.

With a particular focus on the 1% PdFe/ TiO_2 catalyst, we next conducted a series of hot-filtration experiments to identify the contribution of leached metal species to catalytic activity (Table S14). In the absence of the solid catalyst, minimal additional products were observed, with a total product yield of 5.96% after the two-part, 1 h duration, hot-filtration experiment. This value was nearly identical with that observed for the same experiment conducted over the 1% PdFe/ TiO_2 catalyst (5.60%), with the small quantity of additional total products observed partially attributed to the contribution from residual H_2O_2 generated in the initial 0.5 h of the reaction (25 μmol).

To determine if the inactivity observed in the 1% PdFe/ TiO_2 hot-filtration experiment was due to the limited ability of the homogeneous component to synthesize H_2O_2 , a further hot-filtration experiment was conducted whereby, after the initial 0.5 h reaction, the 1% PdFe/ TiO_2 catalyst was replaced with a 1% Pd/ TiO_2 catalyst, ensuring that the total moles of Pd was equal to that in the bimetallic catalyst. Perhaps unexpectedly, a minor improvement in total product yield was observed (7.65%), comparable to the sum of the 1% PdFe/ TiO_2 (5.60%) and 1% Pd/ TiO_2 (1.30%) components when they were used independently over 0.5 h. A similar finding was observed with regard to residual H_2O_2 . Again, the contribution from residual H_2O_2 , (25 μmol), synthesized over the 1% PdFe/ TiO_2 catalyst in the initial 0.5 h experiment, should be considered. It is therefore possible to conclude that the contribution of leached species toward benzyl alcohol oxidation is negligible.

We, along with others, have previously demonstrated the enhanced activity of PdFe catalysts for the oxidative

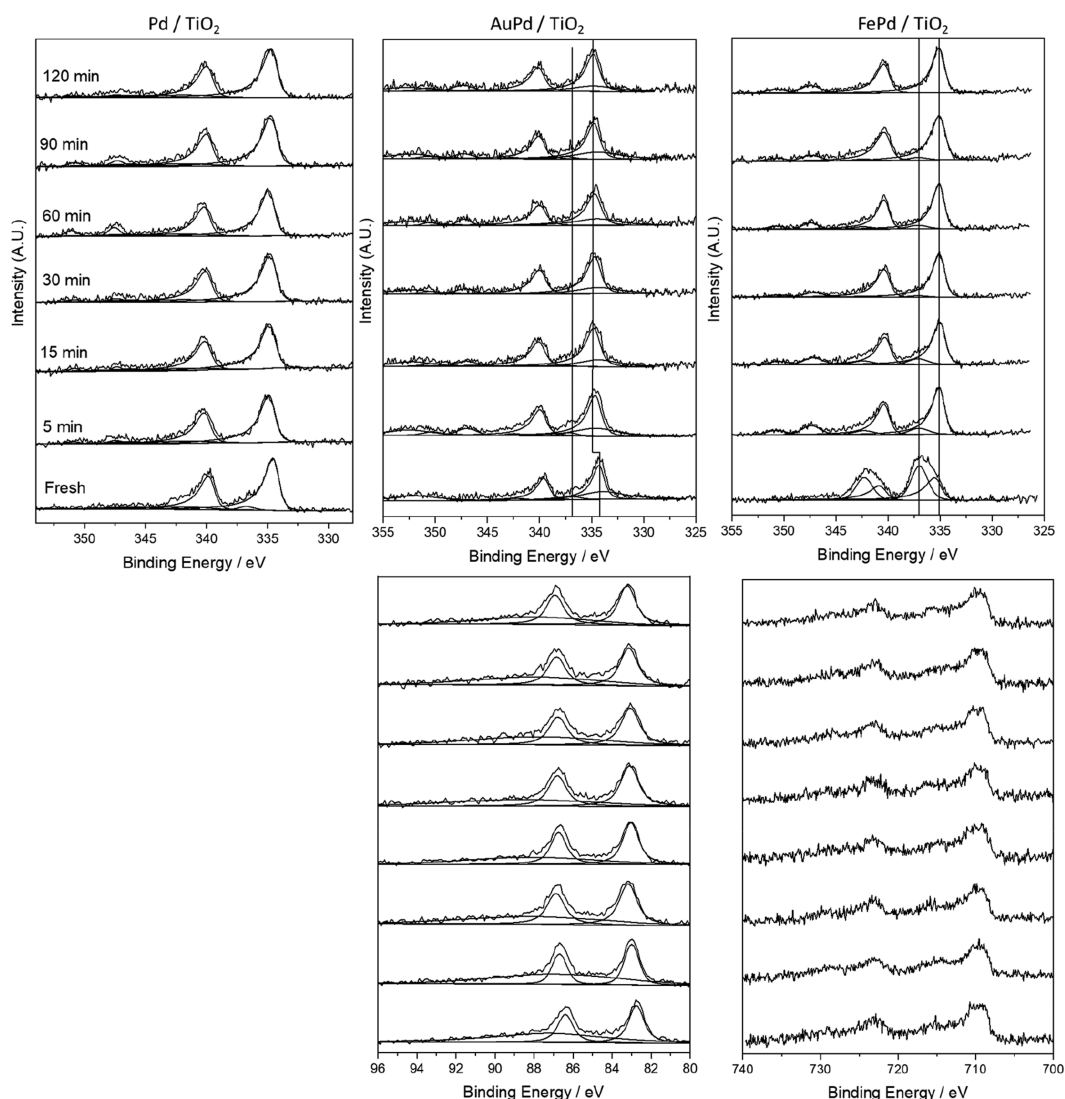


Figure 6. XPS spectra of Pd(3d) regions for the 1% Pd/TiO₂, 1% PdAu/TiO₂, and 1% PdFe/TiO₂ catalysts as a function of reaction time. The Au(4f) and Fe(2p) regions are shown below their respective bimetallic catalysts.

degradation of phenol, through the bifunctionality of the catalyst where the Pd component synthesizes H₂O₂, while the Fe component catalyzes the production of oxygen-based radicals, which are known to be key in achieving high phenol conversion rates.^{69–71} Considering the radical nature of benzyl alcohol oxidation when preformed H₂O₂ is used as an oxidant,¹⁹ we next set out to establish the underlying cause for the enhanced activity of the 1% PdFe/TiO₂ catalyst over its 1% PdAu/TiO₂ and 1% Pd/TiO₂ analogues.

Building on this earlier work,^{69–72} we conducted a series of spin trapping electron paramagnetic resonance (EPR) spectroscopy experiments using 5,5-dimethyl-1-pyrroline *N*-oxide (DMPO) as a spin trap (with control reactions being reported in Figure S6). Figure 8A shows the spectra obtained under typical reaction conditions with the three different catalysts. Spectra i and ii, representing 5 and 30 min reaction times, respectively, were obtained using the 1% Pd/TiO₂ catalyst, with no radicals trapped in solution for this catalyst. In the case of the 1% PdAu/TiO₂ catalyst, spectra iii and iv are for reaction times of 5 and 30 min, respectively, exhibiting a signal that can be attributed to an O-centered methoxy radical trapped by DMPO to form a DMPO-OCH₃ nitroxide radical

adduct with $g_{\text{iso}} = 2.006$, $a_{\text{iso}}(^{14}\text{N}) = 1.373$ mT and $a_{\text{iso}}(^1\text{H}_\beta) = 0.858$ mT, which are in agreement with previously reported hyperfine coupling values.⁷² Methoxy-based radicals (CH₃O•) in the reaction medium are thought to originate from the solvent, i.e. methanol, which are known to act as scavengers for •OH radicals^{73,74} that are formed either during H₂O₂ synthesis or by the catalyzed generation of •OH from the synthesized H₂O₂. It is therefore possible to conclude that the solvent is not benign and that the enhanced activity previously reported by Santonastaso et al.⁸ in using a bimetallic AuPd supported catalyst in a methanol-rich solvent system may not only result from an increased solubility of H₂. Interestingly, in the case of the 1% PdFe/TiO₂ catalyst, the concentration of the DMPO-OCH₃ adduct, at both 5 min contact time (spectrum v) and at 30 min contact time (spectrum vi), is higher in comparison to the 1% PdAu/TiO₂ and 1% Pd/TiO₂ catalysts, correlating well with the benzaldehyde yields. Slight decreases in the concentration of the adducts were also seen over longer contact times, which could be attributed to decomposition of the nitroxide species. A small secondary signal arising from ring opening of the spin trap adduct is also present at long contact times in the case of the 1% PdFe/TiO₂

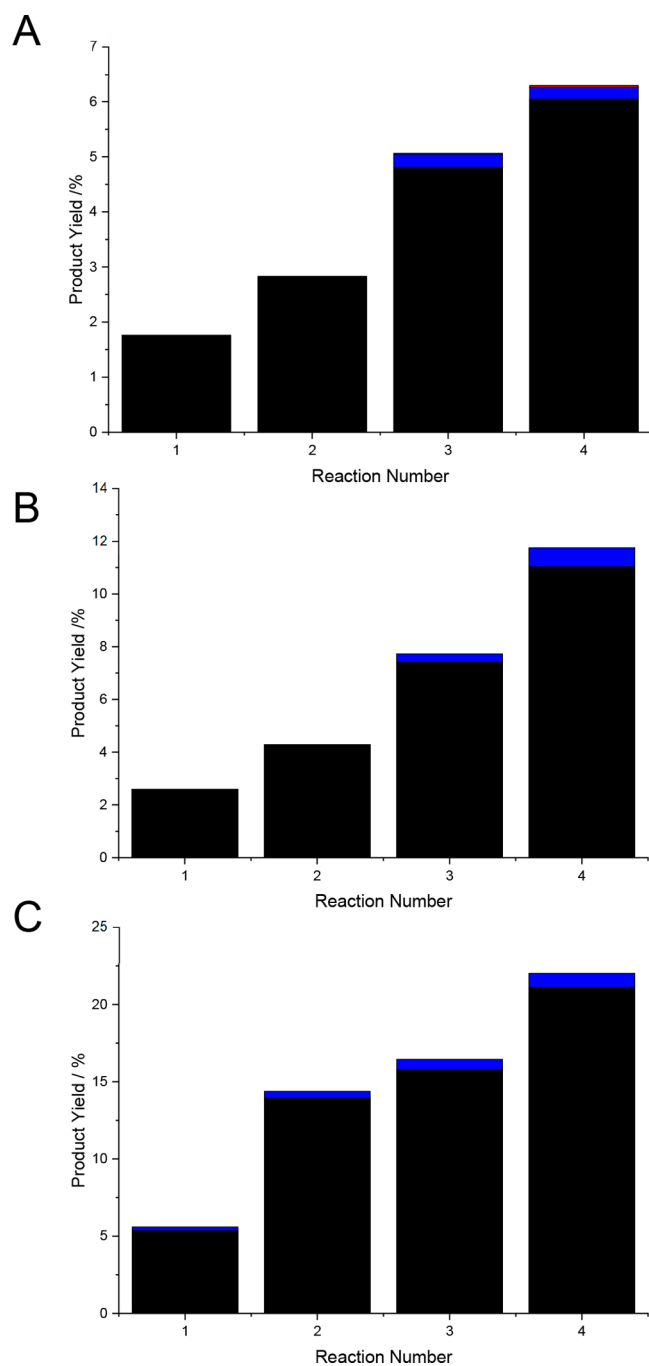


Figure 7. Comparison of the catalytic activity of (A) 1% Pd/TiO₂, (B) 1% PdAu/TiO₂, and (C) 1% PdFe/TiO₂ toward the selective oxidation of benzyl alcohol, via *in situ* H₂O₂ synthesis, over sequential reaction runs. Key: benzaldehyde (black bars), benzoic acid (blue bars). Reaction conditions: catalyst (0.01 g), benzyl alcohol (1.04 g, 9.62 mmol), MeOH (7.1 g), 5% H₂/CO₂ (2.9 MPa), 25% O₂/CO₂ (1.1 MPa), 0.5 h, 50 °C, 1200 rpm. See Table S13 for the product distribution.

catalyst (spectrum vi). This phenomenon has been previously reported in Fenton-like systems.⁷⁵

In order to confirm the proposed hypothetical mechanism and ascertain the nature of the primary radicals generated by the catalytic reaction of H₂ and O₂, a series of spin-trapping experiments were conducted in water (Figure 8B) in the absence of species capable of scavenging •OH and •OOH radicals. Spectra vii and viii were recorded in the absence of

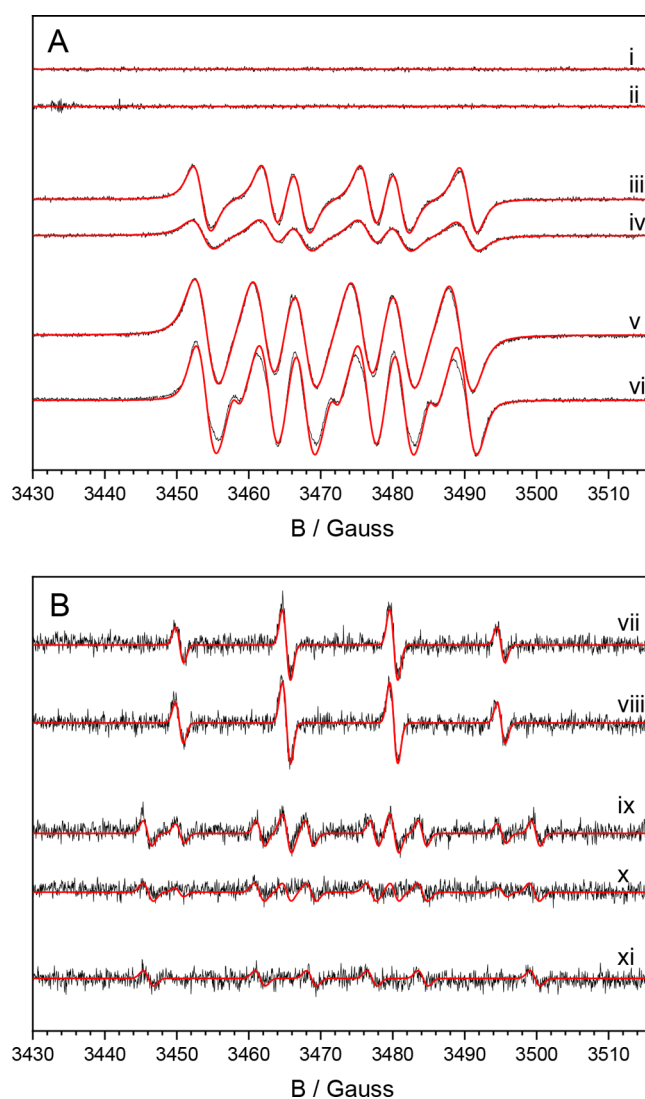


Figure 8. Experimental (black) and simulated (red) EPR spectra of DMPO-radical adducts formed during the oxidation reaction. (A) Reactions conducted in methanol at 50 °C, with benzyl alcohol (9.62 mmol), 5% H₂/CO₂ (2.9 MPa), and 25% O₂/CO₂ (1.1 MPa) in the presence of DMPO and (i) 1%Pd/TiO₂ 5 min reaction, (ii) 1% Pd/TiO₂ 30 min reaction, (iii) 1% PdAu/TiO₂ 5 min reaction, (iv) 1% PdAu/TiO₂ 30 min reaction, (v) 1% PdFe/TiO₂ 5 min reaction, and (vi) 1% PdFe/TiO₂ 30 min reaction. (B) Reactions conducted in water at 50 °C, in the presence of DMPO and (vii) 5% H₂/CO₂ (2.9 MPa), 25% O₂/CO₂ (1.1 MPa), and 1% PdAu/TiO₂, (viii) 5% H₂/CO₂ (2.9 MPa), 25% O₂/CO₂ (1.1 MPa), and 1% PdFe/TiO₂, (ix) benzyl alcohol (9.62 mmol) and 1% PdAu/TiO₂, (x) benzyl alcohol (9.62 mmol) and 1% PdFe/TiO₂, and (xi) benzyl alcohol (9.62 mmol), 5% H₂/CO₂ (2.9 MPa), and 25% O₂/CO₂ (1.1 MPa).

benzyl alcohol, but in the presence of H₂, O₂, and a catalyst, 1% PdAu/TiO₂ (spectrum vii) or 1% PdFe/TiO₂ (spectrum viii). These spectra are dominated by the signal of a DMPO-OH adduct, showing equal hyperfine couplings for the ¹⁴N of the NO• moiety and the β proton, $g_{\text{iso}} = 2.006$, $a_{\text{iso}}(^{14}\text{N}) = 1.493$ mT, and $a_{\text{iso}}(^1\text{H}_\beta) = 1.493$ mT. This signal is symptomatic of •OH and/or •OOH trapping. The DMPO-OOH adduct has a half-life of 1–4 min and decays into DMPO-OH if unreacted DMPO is present;^{76,77} therefore, under these conditions it is not possible to differentiate between •OH and •OOH. Under conditions where no reactant

gases were present, but only benzyl alcohol and the catalyst, 1% PdAu/TiO₂ (spectrum ix) and 1% PdFe/TiO₂ (spectrum x), the concentration of the DMPO-OH adduct significantly decreased, as would be expected. Interestingly, a new signal characterized by $g_{\text{iso}} = 2.006$, $a_{\text{iso}}(^{14}\text{N}) = 1.559$ mT, and $a_{\text{iso}}(^1\text{H}_\beta) = 2.260$ mT and consistent with a DMPO-trapped C-centered PhCH[•](OH) radical was noted.⁶⁶ This is an important observation because it suggests that PhCH[•](OH) is most likely the first intermediate in the radical oxidation of benzyl alcohol. Spectra ix and x also indicate that the catalyst itself without H₂ and O₂ might be responsible for some limited activity, and in these circumstances the amount of radicals trapped when 1% PdAu/TiO₂ was used was higher than that when 1% PdFe/TiO₂ was used. Finally, spectrum xi reports the case of a reaction conducted with benzyl alcohol, H₂, and O₂, in the absence of a catalyst. In perfect agreement with the results described above, no signal from radical reactive oxygen species (ROS) was detected, proving once more that radical ROS generation is a catalytic process. Nevertheless, the spectrum shows a small contribution of trapped PhCH[•](OH) radicals. This is consistent with a small equilibrium amount of H₂O₂ forming from H₂ and O₂ without the presence of a catalyst, which could have oxidized some of the benzyl alcohol present. It is therefore possible to conclude that the ability of Fe to catalyze the disproportionation of synthesized H₂O₂ to ROS, via a Fenton pathway, is key in achieving the enhanced activity observed by the 1% PdFe/TiO₂ catalyst.

CONCLUSIONS

We have demonstrated that it is possible to selectively oxidize benzyl alcohol with high selectivity to benzaldehyde via the *in situ* production of H₂O₂ at temperatures where limited activity is observed with O₂ alone. The incorporation of Fe into a supported 1% Pd/TiO₂ catalyst is seen to dramatically enhance catalytic activity in comparison to either the monometallic Pd or analogous 1% PdAu/TiO₂ catalyst. Furthermore, we show that through continual replacement of the reactant gases it is possible to reach high yields of benzaldehyde, with the 1% PdFe/TiO₂ catalyst achieving yields approximately double those exhibited by the 1% Pd/TiO₂ and 1% PdAu/TiO₂ catalysts. The enhanced activity of the 1% PdFe/TiO₂ catalyst is attributed to the maintenance of domains of mixed Pd oxidation state and the continual low-level production of H₂O₂ over extended reaction times.

EPR analysis revealed that the enhanced activity of the 1% PdFe/TiO₂ catalyst can be correlated with the increased formation of oxygen-based radical species in comparison to 1% PdAu/TiO₂ and 1% Pd/TiO₂ analogues. The formation of methyl-based radicals resulting from the radical scavenging ability of the reaction solvent has also been identified. However, at present we are not able to delineate the contribution to the overall oxidation reaction from the two categories of radical species, but the potential noninnocent nature of the methanol solvent is a crucial observation.

We believe these catalysts represent a promising basis for further exploration, in particular, given their greatly reduced precious-metal content and demonstrated high selectivity to desirable products.

ASSOCIATED CONTENT

Supporting Information

The Supporting Information is available free of charge at <https://pubs.acs.org/doi/10.1021/acscatal.0c04586>.

Catalytic testing data for both the direct synthesis of H₂O₂ and *in situ* oxidation of benzyl alcohol and additional characterization of key materials including transmission electron microscopy, X-ray photoelectron microscopy, energy dispersive X-ray elemental analysis, and surface area determination (PDF)

AUTHOR INFORMATION

Corresponding Authors

Xi Liu – *In-situ Center for Physical Science, School of Chemistry and Chemical Engineering, Shanghai Jiao Tong University, 200240 Shanghai, People's Republic of China;*
Email: Liuxi@sjtu.edu.cn

Graham J. Hutchings – *School of Chemistry, Cardiff University, Cardiff CF10 3AT, United Kingdom;*
orcid.org/0000-0001-8885-1560; Email: Hutch@cardiff.ac.uk

Authors

Caitlin M. Crombie – *School of Chemistry, Cardiff University, Cardiff CF10 3AT, United Kingdom*

Richard J. Lewis – *School of Chemistry, Cardiff University, Cardiff CF10 3AT, United Kingdom;* orcid.org/0000-0001-9990-7064

Rebekah L. Taylor – *School of Chemistry, Cardiff University, Cardiff CF10 3AT, United Kingdom*

David J. Morgan – *School of Chemistry, Cardiff University, Cardiff CF10 3AT, United Kingdom; HarwellXPS, Research Complex at Harwell (RCaH), Didcot OX11 0FA, United Kingdom;* orcid.org/0000-0002-6571-5731

Thomas E. Davies – *School of Chemistry, Cardiff University, Cardiff CF10 3AT, United Kingdom*

Andrea Folli – *School of Chemistry, Cardiff University, Cardiff CF10 3AT, United Kingdom;* orcid.org/0000-0001-8913-6606

Damien M. Murphy – *School of Chemistry, Cardiff University, Cardiff CF10 3AT, United Kingdom;*
orcid.org/0000-0002-5941-4879

Jennifer K. Edwards – *School of Chemistry, Cardiff University, Cardiff CF10 3AT, United Kingdom*

Jizhen Qi – *i-Lab, CAS center for Excellence in Nanoscience, Suzhou Institute of Nano-Tech and Nano-Bionics, Chinese Academy of Sciences, 215123 Suzhou, People's Republic of China*

Haoyu Jiang – *In-situ Center for Physical Science, School of Chemistry and Chemical Engineering, Shanghai Jiao Tong University, 200240 Shanghai, People's Republic of China*

Christopher J. Kiely – *School of Chemistry, Cardiff University, Cardiff CF10 3AT, United Kingdom; Department of Materials Science and Engineering, Lehigh University, Bethlehem, Pennsylvania 18015, United States*

Martin Skov Skjøth-Rasmussen – *Haldor Topsøe A/S, DK-2800 Kongens Lyngby, Denmark*

Complete contact information is available at:
<https://pubs.acs.org/doi/10.1021/acscatal.0c04586>

Author Contributions

[†]C.M.C. and R.J.L. contributed equally to this work.

Notes

The authors declare no competing financial interest.

ACKNOWLEDGMENTS

The authors wish to thank Haldor Topsoe and EPSRC for financial support and the Cardiff University electron microscope facility for the initial transmission electron microscopy work. X.L. thanks the National Natural Science Foundation of China for financial support (21991153, 21991150, 21872163, 22072090). The authors also appreciate the technical support provided by Mr. Hiroaki Matsumoto and Mr. Chaobin Zeng, as well as Hitachi High-Technologies (Shanghai) Co. Ltd for the HR-STEM characterization. XPS data collection was performed at the EPSRC National Facility for XPS ("HarwellXPS"), operated by Cardiff University and UCL, under contract no. PR16195. Information on the data underpinning the results presented here, including how to access them, can be found at <http://doi.org/10.17035/d.2021.0128838559>.

REFERENCES

- (1) Savara, A.; Chan-Thaw, C. E.; Rossetti, I.; Villa, A.; Prati, L. Benzyl Alcohol Oxidation on Carbon-Supported Pd Nanoparticles: Elucidating the Reaction Mechanism. *ChemCatChem* **2014**, *6* (6), 3464–3473.
- (2) Della Pina, C.; Falletta, E.; Rossi, M. Highly selective oxidation of benzyl alcohol to benzaldehyde catalyzed by bimetallic gold-copper catalyst. *J. Catal.* **2008**, *260* (2), 384–386.
- (3) Ryland, B. L.; Stahl, S. S. Practical aerobic oxidations of alcohols and amines with homogeneous copper/TEMPO and related catalyst systems. *Angew. Chem., Int. Ed.* **2014**, *53* (34), 8824–8838.
- (4) Sheldon, R. A. Recent advances in green catalytic oxidations of alcohols in aqueous media. *Catal. Today* **2015**, *247*, 4–13.
- (5) He, Q.; Miedziak, P. J.; Kesavan, L.; Dimitratos, N.; Sankar, M.; Lopez-Sanchez, J. A.; Forde, M. M.; Edwards, J. K.; Knight, D. W.; Taylor, S. H.; Kiely, C. J.; Hutchings, G. J. Switching-off toluene formation in the solvent-free oxidation of benzyl alcohol using supported trimetallic Au-Pd-Pt nanoparticles. *Faraday Discuss.* **2013**, *162*, 365–378.
- (6) Wu, P.; Cao, Y.; Zhao, L.; Wang, Y.; He, Z.; Xing, W.; Bai, P.; Mintova, S.; Yan, Z. Formation of PdO on Au-Pd bimetallic catalysts and the effect on benzyl alcohol oxidation. *J. Catal.* **2019**, *375*, 32–43.
- (7) Enache, D. I.; Barker, D.; Edwards, J. K.; Taylor, S. H.; Knight, D. W.; Carley, A. F.; Hutchings, G. J. Solvent-free oxidation of benzyl alcohol using titania-supported gold-palladium catalysts: Effect of Au-Pd ratio on catalytic performance. *Catal. Today* **2007**, *122* (3), 407–411.
- (8) Santonastaso, M.; Freakley, S. J.; Miedziak, P. J.; Brett, G. L.; Edwards, J. K.; Hutchings, G. J. Oxidation of benzyl alcohol using in situ generated hydrogen peroxide. *Org. Process Res. Dev.* **2014**, *18* (11), 1455–1460.
- (9) Göksu, H.; Burhan, H.; Mustafov, S. D.; Şen, F. Oxidation of benzyl alcohol compounds in the presence of carbon hybrid supported platinum nanoparticles (Pt@CHs) in oxygen atmosphere. *Sci. Rep.* **2020**, *10* (1), 5439.
- (10) Savara, A.; Rossetti, I.; Chan-Thaw, C. E.; Prati, L.; Villa, A. Microkinetic Modeling of Benzyl Alcohol Oxidation on Carbon-Supported Palladium Nanoparticles. *ChemCatChem* **2016**, *8* (8), 2482–2491.
- (11) Kawamura, K.; Yasuda, T.; Hatanaka, T.; Hamahiga, K.; Matsuda, N.; Ueshima, M.; Nakai, K. Oxidation of aliphatic alcohols and benzyl alcohol by H₂O₂ under the hydrothermal conditions in the presence of solid-state catalysts using batch and flow reactors. *Chem. Eng. J.* **2016**, *285*, 49–56.
- (12) Hou, W.; Dehm, N. A.; Scott, R. W. J. Alcohol oxidations in aqueous solutions using Au, Pd, and bimetallic AuPd nanoparticle catalysts. *J. Catal.* **2008**, *253* (1), 22–27.
- (13) Hutchings, G. J.; Kiely, C. J. Strategies for the synthesis of supported gold palladium nanoparticles with controlled morphology and composition. *Acc. Chem. Res.* **2013**, *46* (46), 1759–1772.
- (14) Xu, C.; Zhang, L.; An, Y.; Wang, X.; Xu, G.; Chen, Y.; Dai, L. Promotional synergistic effect of Sn doping into a novel bimetallic Sn-W oxides/graphene catalyst for selective oxidation of alcohols using aqueous H₂O₂ without additives. *Appl. Catal., A* **2018**, *558*, 26–33.
- (15) Cánepa, A. L.; Elías, V. R.; Vaschetti, V. M.; Sabre, E. V.; Eimer, G. A.; Casuscelli, S. G. Selective oxidation of benzyl alcohol through eco-friendly processes using mesoporous V-MCM-41, Fe-MCM-41 and Co-MCM-41 materials. *Appl. Catal., A* **2017**, *545*, 72–78.
- (16) Kamonsatikul, C.; Khamnaen, T.; Phiriyawirut, P.; Charoenchaidet, S.; Somsook, E. Synergistic activities of magnetic iron-oxide nanoparticles and stabilizing ligands containing ferrocene moieties in selective oxidation of benzyl alcohol. *Catal. Commun.* **2012**, *26*, 1–5.
- (17) Shi, F.; Tse, M. K.; Pohl, M.-M.; Brückner, A.; Zhang, S.; Beller, M. Tuning catalytic activity between homogeneous and heterogeneous catalysis: Improved activity and selectivity of free nano-Fe₃O₄ in selective oxidations. *Angew. Chem., Int. Ed.* **2007**, *46* (46), 8866–8868.
- (18) Zhang, J.; Xiao, S.; Chen, R.; Chen, F. Promotional effect of short-chain saturated alcohols on Fe₃O₄-catalyzed decomposition of H₂O₂ and its application in selective oxidation of benzyl alcohol. *J. Chem. Technol. Biotechnol.* **2019**, *94* (5), 1613–1621.
- (19) Zhao, Y.; Yu, C.; Wu, S.; Zhang, W.; Xue, W.; Zeng, Z. Synthesis of benzaldehyde and benzoic acid by selective oxidation of benzyl alcohol with iron(III) tosylate and hydrogen peroxide: A solvent-controlled reaction. *Catal. Lett.* **2018**, *148* (10), 3082–3092.
- (20) Scoville, J. R.; Novicova, J. I. A. (Cottrell Ltd.) US 5900256, 1996.
- (21) Blaser, B.; Worms, K.-H.; Schiefer, J. (Henkel AG and Co KGaA) US 3122417A, 1959.
- (22) Moreno, I.; Dummer, N. F.; Edwards, J. K.; Alhumaimess, M.; Sankar, M.; Sanz, R.; Pizarro, P.; Serrano, D. P.; Hutchings, G. J. Selective oxidation of benzyl alcohol using in-situ generated H₂O₂ over hierarchical Au-Pd titanium silicalite catalysts. *Catal. Sci. Technol.* **2013**, *3* (9), 2425–2434.
- (23) Torrente-Murciano, L.; Villager, T.; Chadwick, D. Selective oxidation of salicylic alcohol to aldehyde with O₂/H₂ using Au-Pd on titanate nanotube catalysts. *ChemCatChem* **2015**, *7* (6), 925–927.
- (24) Santos, A.; Lewis, R. J.; Malta, G.; Howe, A. G. R.; Morgan, D. J.; Hampton, E.; Gaskin, P.; Hutchings, G. J. Direct synthesis of hydrogen peroxide over Au-Pd supported nanoparticles under ambient conditions. *Ind. Eng. Chem. Res.* **2019**, *58* (28), 12623–12631.
- (25) Edwards, J. K.; Solsona, B.; N, E. N.; Carley, A. F.; Herzing, A. A.; Kiely, C. J.; Hutchings, G. J. Switching off hydrogen peroxide hydrogenation in the direct synthesis process. *Science* **2009**, *323* (5917), 1037–1041.
- (26) Savara, A.; Chan-Thaw, C. E.; Sutton, J. E.; Wang, D.; Prati, L.; Alberto, V. Molecular Origin of the Selectivity Differences between Palladium and Gold-Palladium in Benzyl Alcohol Oxidation: Different Oxygen Adsorption Properties. *ChemCatChem* **2017**, *9* (2), 253–257.
- (27) Wilson, N. M.; Priyadarshini, P.; Kunz, S.; Flaherty, D. W. Direct synthesis of H₂O₂ on Pd and Au_xPd_{1-x} clusters: Understanding the effects of alloying Pd with Au. *J. Catal.* **2018**, *357* (357), 163–175.
- (28) Bonnard, J.; Poilane, G. (Rhone Poulenc SA) US 3387036A, 1968.
- (29) Sankar, M.; He, Q.; Morad, M.; Pritchard, J.; Freakley, S. J.; Edwards, J. K.; Taylor, S. H.; Morgan, D. J.; Carley, A. F.; Knight, D. W.; Kiely, C. J.; Hutchings, G. J. Synthesis of stable ligand-free gold-palladium nanoparticles using a simple excess anion method. *ACS Nano* **2012**, *6* (8), 6600–6613.
- (30) Edwards, J. K.; Thomas, A.; Carley, A. F.; Herzing, A. A.; Kiely, C. J.; Hutchings, G. J. Au-Pd supported nanocrystals as catalysts for the direct synthesis of hydrogen peroxide from H₂ and O₂. *Green Chem.* **2008**, *10* (4), 388–394.
- (31) Crole, D. A.; Freakley, S. J.; Edwards, J. K.; Hutchings, G. J. Direct synthesis of hydrogen peroxide in water at ambient temperature. *Proc. R. Soc. London, Ser. A* **2016**, *472*, 20160156.

- (32) Gemo, N.; Biasi, P.; Salmi, T. O.; Canu, P. H₂ solubility in methanol in the presence of CO₂ and O₂. *J. Chem. Thermodyn.* **2012**, *54*, 1–9.
- (33) Stoll, S.; Schweiger, A. EasySpin, a comprehensive software package for spectral simulation and analysis in EPR. *J. Magn. Reson.* **2006**, *178* (1), 42–55.
- (34) Arrigo, R.; Schuster, M. E.; Abate, S.; Giorgianni, G.; Centi, G.; Perathoner, S.; Wrabetz, S.; Pfeifer, V.; Antonietti, M.; Schlögl, R. Pd Supported on carbon nitride boosts the direct hydrogen peroxide synthesis. *ACS Catal.* **2016**, *6* (10), 6959–6966.
- (35) Arrigo, R.; Schuster, M. E.; Abate, S.; Wrabetz, S.; Amakawa, K.; Teschner, D.; Freni, M.; Centi, G.; Perathoner, S.; Hävecker, M.; Schlögl, R. Dynamics of palladium on nanocarbon in the direct synthesis of H₂O₂. *ChemSusChem* **2014**, *7* (1), 179–194.
- (36) Liu, Q.; Bauer, J. C.; Schaak, R. E.; Lunsford, J. H. Supported palladium nanoparticles: an efficient catalyst for the direct formation of H₂O₂ from H₂ and O₂. *Angew. Chem., Int. Ed.* **2008**, *47* (33), 6221–6224.
- (37) Flaherty, D. W. Direct Synthesis of H₂O₂ from H₂ and O₂ on Pd Catalysts: Current Understanding, Outstanding Questions, and Research Needs. *ACS Catal.* **2018**, *8*, 1520–1527.
- (38) Wilson, N. M.; Flaherty, D. W. Mechanism for the Direct Synthesis of H₂O₂ on Pd Clusters: Heterolytic Reaction Pathways at the Liquid-Solid Interface. *J. Am. Chem. Soc.* **2016**, *138* (138), 574–586.
- (39) Lewis, R. J.; Hutchings, G. J. Recent Advances in the Direct Synthesis of H₂O₂. *ChemCatChem* **2019**, *11* (11), 298–308.
- (40) Costa, R. C. C.; Lelis, M. F. F.; Oliveira, L. C. A.; Fabris, J. D.; Ardisson, J. D.; Rios, R. R. V. A.; Silva, C. N.; Lago, R. M. Novel active heterogeneous Fenton system based on Fe_{3-x}M_xO₄ (Fe, Co, Mn, Ni): The role of M²⁺ species on the reactivity towards H₂O₂ reactions. *J. Hazard. Mater.* **2006**, *129* (1), 171–178.
- (41) Enache, D. I.; Edwards, J. K.; Landon, P.; Solsona-Espriu, B.; Carley, A. F.; Herzing, A. A.; Watanabe, M.; Kiely, C. J.; Knight, D. W.; Hutchings, G. J. Solvent-free oxidation of primary alcohols to aldehydes using Au-Pd/TiO₂ catalysts. *Science* **2006**, *311* (5759), 362–365.
- (42) Tang, C.; Zhang, N.; Shao, Q.; Huang, X.; Xiao, X. Rational design of ordered Pd-Pb nanocubes as highly active, selective and durable catalysts for solvent-free benzyl alcohol oxidation. *Nanoscale* **2019**, *11* (12), 5145–5150.
- (43) Edwards, J.; Solsona, B.; Landon, P.; Carley, A.; Herzing, A.; Kiely, C.; Hutchings, G. Direct synthesis of hydrogen peroxide from H₂ and O₂ using TiO₂-supported Au-Pd catalysts. *J. Catal.* **2005**, *236* (1), 69–79.
- (44) Lewis, R. J.; Ueura, K.; Fukuta, Y.; Freakley, S. J.; Kang, L.; Wang, R.; He, Q.; Edwards, J. K.; Morgan, D. J.; Yamamoto, Y.; Hutchings, G. J. The direct synthesis of H₂O₂ using TS-1 supported catalysts. *ChemCatChem* **2019**, *11* (6), 1673–1680.
- (45) Chen, M.; Kumar, D.; Yi, C.-W.; Goodman, D. W. The promotional effect of gold in catalysis by palladium-gold. *Science* **2005**, *310* (5746), 291–293.
- (46) Freakley, S. J.; He, Q.; Harry, J. H.; Lu, L.; Crole, D. A.; Morgan, D. J.; Ntainjua, E. N.; Edwards, J. K.; Carley, A. F.; Borisevich, A. Y.; Kiely, C. J.; Hutchings, G. J. Palladium-tin catalysts for the direct synthesis of H₂O₂ with high selectivity. *Science* **2016**, *351* (6276), 965–968.
- (47) Zhang, J.; Shao, Q.; Zhang, Y.; Bai, S.; Feng, Y.; Huang, X. Promoting the direct H₂O₂ generation catalysis by using hollow Pd-Sn intermetallic nanoparticles. *Small* **2018**, *14* (16), 1703990–1703997.
- (48) Wang, S.; Gao, K.; Li, W.; Zhang, J. Effect of Zn addition on the direct synthesis of hydrogen peroxide over supported palladium catalysts. *Appl. Catal., A* **2017**, *531*, 89–95.
- (49) Gu, J.; Wang, S.; He, Z.; Han, Y.; Zhang, J. Direct synthesis of hydrogen peroxide from hydrogen and oxygen over activated-carbon-supported Pd-Ag alloy catalysts. *Catal. Sci. Technol.* **2016**, *6* (3), 809–817.
- (50) Tian, P.; Xu, X.; Ao, C.; Ding, D.; Li, W.; Si, R.; Tu, W.; Xu, J.; Han, Y. Direct and selective synthesis of hydrogen peroxide over palladium-tellurium catalysts at ambient pressure. *ChemSusChem* **2017**, *10* (17), 3342–3346.
- (51) Maity, S.; Eswaramoorthy, M. Ni-Pd bimetallic catalysts for the direct synthesis of H₂O₂ - unusual enhancement of Pd activity in the presence of Ni. *J. Mater. Chem. A* **2016**, *4* (9), 3233–3237.
- (52) Crole, D. A.; Underhill, R.; Edwards, J. K.; Shaw, G.; Freakley, S. J.; Hutchings, G. J.; Lewis, R. J. The direct synthesis of hydrogen peroxide from H₂ and O₂ using PdNi/TiO₂ catalysts. *Philos. Trans. R. Soc., A* **2020**, *378* (2176), 20200062.
- (53) Wang, Y.; Pan, H.; Lin, Q.; Shi, Y.; Zhang, J. Synthesis of Pd-M@HCS (M = Co, Ni, Cu) bimetallic catalysts and their catalytic performance for direct synthesis of H₂O₂. *Catalysts* **2020**, *10* (3), 303–315.
- (54) Wang, S.; Lewis, R. J.; Doronkin, D. E.; Morgan, D. J.; Grunwaldt, J.; Hutchings, G. J.; Behrens, S. The direct synthesis of hydrogen peroxide from H₂ and O₂ using Pd-Ga and Pd-In catalysts. *Catal. Sci. Technol.* **2020**, *10*, 1925–1932.
- (55) Choudhary, V. R.; Gaikwad, A. G.; Sansare, S. D. Activation of supported Pd metal catalysts for selective oxidation of hydrogen to hydrogen peroxide. *Catal. Lett.* **2002**, *83* (3–4), 235–239.
- (56) Gaikwad, A. G.; Sansare, S. D.; Choudhary, V. R. Direct oxidation of hydrogen to hydrogen peroxide over Pd-containing fluorinated or sulfated Al₂O₃, ZrO₂, CeO₂, ThO₂, Y₂O₃ and Ga₂O₃ catalysts in stirred slurry reactor at ambient conditions. *J. Mol. Catal. A: Chem.* **2002**, *181* (1–2), 143–149.
- (57) Blanco-Brieva, G.; Cano-Serrano, E.; Campos-Martin, J. M.; Fierro, J. L. G. Direct synthesis of hydrogen peroxide solution with palladium-loaded sulfonic acid polystyrene resins. *Chem. Commun.* **2004**, No. 10, 1184–1185.
- (58) Ouyang, L.; Tian, P.; Da, G.; Xu, X.; Ao, C.; Chen, T.; Si, R.; Xu, J.; Han, Y. The origin of active sites for direct synthesis of H₂O₂ on Pd/TiO₂ catalysts: Interfaces of Pd and PdO domains. *J. Catal.* **2015**, *321*, 70–80.
- (59) Gong, X.; Lewis, R. J.; Zhou, S.; Morgan, D. J.; Davies, T. E.; Liu, X.; Kiely, C. J.; Zong, B.; Hutchings, G. J. Enhanced catalyst selectivity in the direct synthesis of H₂O₂ through Pt incorporation into TiO₂ supported AuPd catalysts. *Catal. Sci. Technol.* **2020**, *10*, 4635–4644.
- (60) Kim, S.; Lee, D.-W.; Lee, K.-Y.; Cho, E. A. Effect of Pd particle size on the direct synthesis of hydrogen peroxide from hydrogen and oxygen over Pd core-porous SiO₂ shell catalysts. *Catal. Lett.* **2014**, *144* (5), 905–911.
- (61) Tian, P.; Ding, D.; Sun, Y.; Xuan, F.; Xu, X.; Xu, J.; Han, Y. Theoretical study of size effects on the direct synthesis of hydrogen peroxide over palladium catalysts. *J. Catal.* **2019**, *369*, 95–104.
- (62) Ma, C. Y.; Dou, B. J.; Li, J. J.; Cheng, J.; Hu, Q.; Hao, Z. P.; Qiao, S. Z. Catalytic oxidation of benzyl alcohol on Au or Au-Pd nanoparticles confined in mesoporous silica. *Appl. Catal., B* **2009**, *92* (1), 202–208.
- (63) Meher, S.; Rana, K. R. A rational design of a Pd-based catalyst with a metal-metal oxide interface influencing molecular oxygen in the aerobic oxidation of alcohols. *Green Chem.* **2019**, *21*, 2494–2503.
- (64) Zhang, Q.; Deng, W.; Wang, Y. Effect of size of catalytically active phases in the dehydrogenation of alcohols and the challenging selective oxidation of hydrocarbons. *Chem. Commun.* **2011**, *47* (33), 9275–9292.
- (65) Wang, H.; Gu, X.; Zheng, X.; Pan, H.; Zhu, J.; Chen, S.; Cao, L.; Li, W.; Lu, J. Disentangling the size-dependent geometric and electronic effects of palladium nanocatalysts beyond selectivity. *Sci. Adv.* **2019**, *5* (5), eaat6413.
- (66) Sankar, M.; Nowicka, E.; Carter, E.; Murphy, D. M.; Knight, D. W.; Bethell, D.; Hutchings, G. J. The benzaldehyde oxidation paradox explained by the interception of peroxy radical by benzyl alcohol. *Nat. Commun.* **2014**, *5* (1), 3332.
- (67) Partenheimer, W. The high yield synthesis of benzaldehydes from benzylic alcohols using homogeneously catalyzed aerobic oxidation in acetic acid. *Adv. Synth. Catal.* **2006**, *348* (4–5), 559–568.

- (68) Liu, Q.; Lunsford, J. H. Controlling factors in the direct formation of H₂O₂ from H₂ and O₂ over a Pd/SiO₂ catalyst in ethanol. *Appl. Catal., A* **2006**, *314* (1), 94–100.
- (69) Underhill, R.; Lewis, R. J.; Freakley, S. J.; Douthwaite, M.; Miedziak, P. J.; Akdim, O.; Edwards, J. K.; Hutchings, G. J. Oxidative degradation of phenol using in-situ generated H₂O₂ combined with Fenton's process. *Johnson Matthey Technol. Rev.* **2018**, *62*, 417–425.
- (70) Triki, M.; Contreras, S.; Medina, F. Pd-Fe/TiO₂ catalysts for phenol degradation with in situ generated H₂O₂. *J. Sol-Gel Sci. Technol.* **2014**, *71* (1), 96–101.
- (71) Yalfani, M. S.; Contreras, S.; Medina, F.; Sueiras, J. Phenol degradation by Fenton's process using catalytic in situ generated hydrogen peroxide. *Appl. Catal., B* **2009**, *89* (3), 519–526.
- (72) Buettner, G. R. Spin Trapping: ESR parameters of spin adducts 1474 1528V. *Free Radical Biol. Med.* **1987**, *3* (4), 259–303.
- (73) Billany, M. R.; Khatib, K.; Gordon, M.; Sugden, J. K. Alcohols and ethanolamines as hydroxyl radical scavengers. *Int. J. Pharm.* **1996**, *137* (2), 143–147.
- (74) Anbar, M.; Meyerstein, D.; Neta, P. Reactivity of aliphatic compounds towards hydroxyl radicals. *J. Chem. Soc. B* **1966**, No. 0, 742–747.
- (75) Makino, K.; Hagiwara, T.; Imaishi, H.; Nishi, M.; Fujii, S.; Ohya, H.; Murakami, A. Dmpo spin trapping in the presence of Fe ion. *Free Radical Res. Commun.* **1990**, *9* (3–6), 233–240.
- (76) Finkelstein, E.; Rosen, G. M.; Rauckman, E. J. Production of hydroxyl radical by decomposition of superoxide spin-trapped adducts. *Mol. Pharmacol.* **1982**, *21* (2), 262–265.
- (77) Finkelstein, E.; Rosen, G. M.; Rauckman, E. J.; Paxton, J. Spin trapping of superoxide. *Mol. Pharmacol.* **1979**, *16* (2), 676–685.